

Process Improvement in the Production of a Pharmaceutical Intermediate Using a Reaction Calorimeter for Studies on the Reaction Kinetics of Amination of a Bromopropyl Compound

Takahiro Sano,* Toru Sugaya, and Masaji Kasai

Sakai Research Laboratories, Kyowa Hakko Kogyo Co., Ltd., 1-1-53 Takasu-Cho, Sakai-City, Osaka, 590, Japan

Abstract:

A synthetic process to produce a pharmaceutical intermediate, [3-(dimethylamino)propyl]triphenylphosphonium bromide (**1**), was established in the laboratory. Process safety evaluations did not show any severe problems. In order to scale up to plant scale, we simulated the reaction for both heat production and byproduct production profiles with kinetic parameters. The kinetic parameters were obtained by laboratory experiments and reaction calorimeter measurements. Under the established conditions, the production operated in a safe manner with high quality.

Introduction

A pharmaceutical intermediate, [3-(dimethylamino)propyl]triphenylphosphonium bromide (**1**), has been synthesized from (3-bromopropyl)triphenylphosphonium bromide (**2**) and dimethylamine (Figure 1)¹. The process flow diagram is shown in Figure 2. The solid of **2** in the solvent (methanol) gradually dissolves during the addition of aqueous dimethylamine and is completely dissolved at the end of the addition. The conversion of the starting material **2** was quantitative, and the isolated yield of **1** was over 90%; however, a small amount (about 1% at 30 °C) of dimeric byproduct **3** was produced (Figure 3), which was difficult to remove in the purification step.

For the commercial production of **1**, it was planned to carry out the process on a 2 m³ scale, so this process could be assessed from a scale-up point of view. We evaluated it for thermal safety as well as control of byproduct formation, and we studied the reaction kinetics in order to determine the best conditions for plant scale production.

Results and Discussion

Safety Evaluation of the Process. From the MSDS (material safety data sheets), there were no toxicity and explosiveness problems with regard to the starting materials and the product. On the basis of the CHETAH² calculation, the plosive hazard classifications (maximum heat of decom-



Figure 1. Synthesis of [3-(dimethylamino)propyl]triphenylphosphonium bromide (**1**).

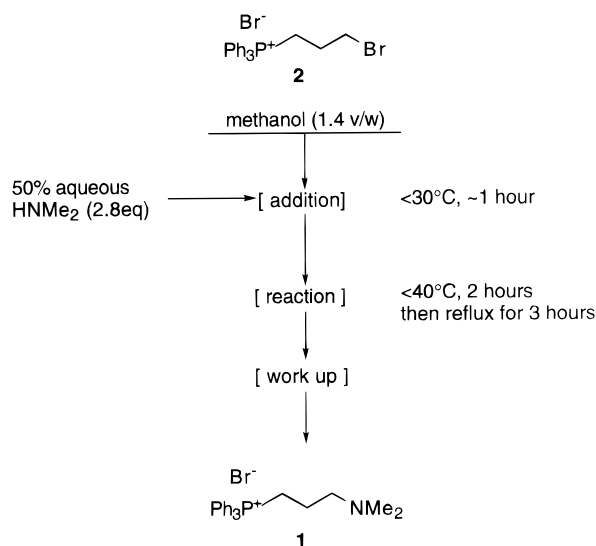


Figure 2. Process flow diagram of synthesis **1**.

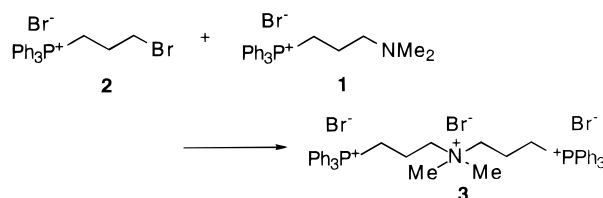


Figure 3. Subreaction to produce the dimeric byproduct **3**.

position, oxygen balance, and so on) of all of the compounds were ranked “low”.

The results of the differential scanning calorimeter (DSC) analysis showed that there was no exothermic decomposition till 200 °C with the starting materials **2** and **3**, and the quantities of heat were less than 400 J/g. From the results of the accelerating rate calorimeter (ARC) analysis, the observed onset temperatures of **1** and **2** were also over 200 °C although thermal inertia factors (PHI factors) were less than 5 (1.7–3.9). These materials were therefore unlikely to present thermal instability hazards at the proposed plant operating temperature.

Next, the process safety was evaluated using a reaction calorimeter (RC1). The heat of the reaction was measured

* Corresponding author. Phone: +81-722-23-5545. Fax: +81-722-27-7214. E-Mail: takahiro.sano@kyowa.co.jp.

(1) (a) Oshima, E.; Kumazawa, T.; Ohtaki, S.; Obase, H.; Ohmori, K.; Ishii, H.; Manabe, H.; Tamura, T.; Shuto, K. Eur. Patent EP 235796, 1987. (b) Corey, E. J.; Desai, C. *Tetrahedron Lett.* **1985**, 26, 5747. (c) Satzinger, G.; Fritsch, E.; Herrman, M. Ger. Patent DE 3248094, 1984. (d) Tretter, J. R. U.S. Patent US 3509175, 1969.

(2) ASTM Subcommittee. *The ASTM CHETAH Version 7.0*; The Computer Program for Chemical Thermodynamic and Energy Release Evaluation; ASTM Data Series DS51B: Philadelphia, 1994.

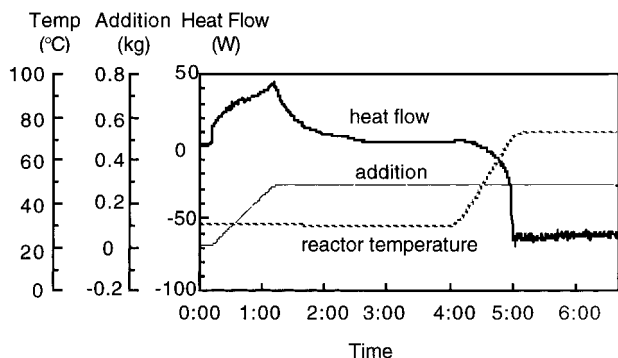


Figure 4. Heat flow of the reaction: bold line (—), heat flow; normal line (—), dimethylamine addition; dashed line (---), temperature of the reactor.

to be 93.6 kJ/mol during the addition of dimethylamine (at 30 °C) and 56.4 kJ/mol after the addition (Figure 4). The heat flow curve dropped under zero base line during and after the temperature ramp. We thought that this phenomenon was caused by heat loss from the cover of the reactor,³ and we measured the heat flow with mixed methanol and aqueous dimethylamine (without **1**) under the same temperature conditions. Comparing these results, there was no heat during both the heating up and refluxing periods. The entire heat of reaction was 150.0 kJ/mol, and the adiabatic temperature rise (ΔT_{ad}) was calculated as about 40 °C on the basis of the reaction mass and the heat capacity of the reactants.

Even when this reaction was performed with the reaction calorimeter at a higher temperature (55 °C) or under adiabatic conditions, the heat of the reaction did not increase (almost 150 kJ/mol) and the maximum temperature increase under adiabatic conditions (from 30 °C) was 37.0 °C (data not shown). The maximum temperature was 67 °C (30 + 37 = 67 °C), but the boiling point of the reactant was 72 °C (aqueous methanol), and reflux did not occur. From these results, this process was judged to be safe, and it was thought that no runaway reaction would occur even in the case of an incorrect reaction temperature or a cooling failure. But at higher temperatures (including adiabatic conditions), byproduct **3** production was increased more than under normal conditions (0.6% at 25 °C and 7.3% at 55 °C).

Kinetics Studies. The addition period and the addition/reaction temperature affected the yield and quality of the product **1**, so we studied the reaction kinetics.

This reaction contains a main reaction (produces **1**) and a subreaction (produces **3**). The substrate **2** reacts through the main reaction and the subreaction (parallel reaction), and the product **1** further reacts through the subreaction (serial reaction). This type of reaction is a so-called serial-parallel reaction (Chart 1).

At first, the reaction was performed under isothermal conditions (25–50 °C) as described in the Experimental Section and the main reaction rate constants (k_{main}) were obtained. The kinetic parameters were calculated from the

Chart 1. Kinetic equations of this process (serial-parallel reaction)^a

$$\frac{dC_2}{dt} = -k_{main}C_2C_{HNMMe_2} - k_{sub}C_1C_2$$

$$\frac{dC_{HNMMe_2}}{dt} = -k_{main}C_2C_{HNMMe_2}$$

$$\frac{dC_1}{dt} = k_{main}C_2C_{HNMMe_2} - k_{sub}C_1C_2$$

$$\frac{dC_3}{dt} = k_{sub}C_1C_2$$

^a C is the concentration of the material (the subscript indicates the compound), t is the reaction time, k_{main} is the reaction constant of the main reaction (product **1**), and k_{sub} is that of the subreaction (product **3**).

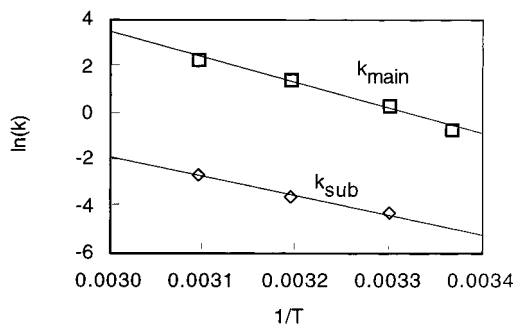


Figure 5. Arrhenius plot of the rate constants obtained from isothermal reaction conditions: k_{main} shows the main reaction, and k_{sub} shows the subreaction.

Table 1. Arrhenius regression analysis results of k_{main} and k_{sub}

	param	value	correlation coeff
k_{main}	E_a	132.5 kJ/mol	0.9886
	A_0	4.68×10^{15} L/mol·h	
k_{sub}	E_a	101.6 kJ/mol	0.9837
	A_0	1.00×10^{10} L/mol·h	

Arrhenius plot. The subreaction rate constants and parameters were then obtained by the reaction of **1** and **2** under isothermal conditions (Figure 5; Table 1). The Arrhenius expressions fitted very well with the observed data ($r^2 > 0.98$).

Modification of the Rate Parameters with Heat Flow. Generally, considering that the heat production is proportional to the conversion, the heat production profile could be calculated using the reaction kinetic parameters. In this process, the subreaction is 20–70 times slower than the main reaction ($k_{main} \gg k_{sub}$) as shown in Figure 5, and the heat production would be estimated only by considering the main reaction.

In scale-up production, it seems difficult to keep the reaction isothermal during the rapid addition of aqueous dimethylamine, which would need about a 2 h addition period (to be mentioned later). At first, we studied the reaction under 30 °C isothermal conditions with a 1 h addition period, and we compared the heat production profile simulated with kinetic parameters and the actual heat production measured by the reaction calorimeter. Obviously, there was a difference, as shown in Figure 6.

(3) The heat flow curve dropped under the zero base line during and after the temperature ramp. This phenomenon was caused by heat loss from the upper cover of the reactor and not by the endotherm: Operating instructions of Reflux and Distillation Set, Mettler Toledo Instrument, 1989.

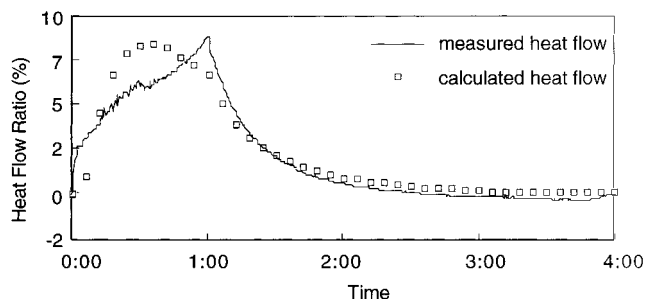


Figure 6. Heat flow measured with the reaction calorimeter. The measured heat flow under 30 °C isothermal conditions with a 1 h addition period is represented by the solid line (—), and the calculated heat flow under the same conditions is represented by boxes (□). The total heat of the reaction (about 150 kJ/mol) is distributed on the basis of the reaction rate.

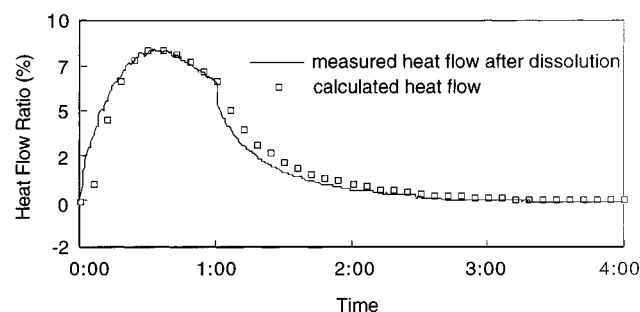


Figure 7. Heat flow measured after the dissolution of **2**: solid line (—), measured heat flow; boxes (□), calculated heat flow.

In this reaction, **2** did not dissolve during the early stage, but it dissolved gradually during the addition period. This dissolution mode of **2** was thought to be one reason for the difference that appeared in Figure 6. We then measured the heat profile with the reaction calorimeter after dissolving **2** with more methanol.⁴ The actual measurement result showed a good agreement with the simulated profile based on the reaction rate (Figure 7). In this case, the evaluation of the heat production calculation using the parameters listed in Table 1 showed high reliability.

On the other hand, these results also proved that the dissolution of **2** was important for considering the heat production, and during the early period of this reaction, the rate-determining step seemed to be the dissolution of **2**. If so, the measured heat flow curve showed the dissolution rate and we intended to clarify the entire reaction from these aspects.

If there would be some mechanical factors influencing the dissolution of **2**, the time to dissolution might change with stirring speed. The stirring speed of the calorimeter was changed in the range 100–300 rpm, and heat flows were measured, but they gave almost the same pattern (Figure 8). Thus, the dissolution was not affected by agitation. By the way, the composition of the reaction solvent changed during the addition of aqueous dimethylamine (initially, the solvent was only methanol; however, during the addition, the water

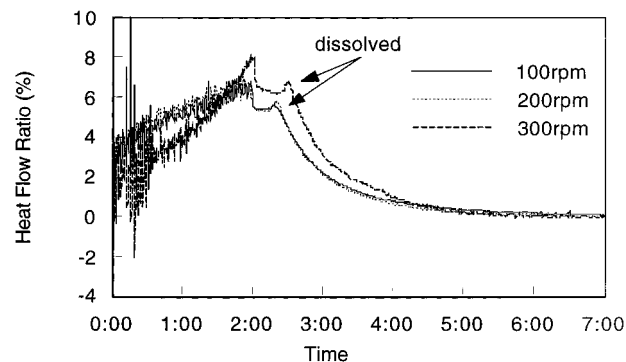


Figure 8. Heat flow curves measured for various stirring speeds at 30 °C with a 2 h period of addition of aqueous dimethylamine.

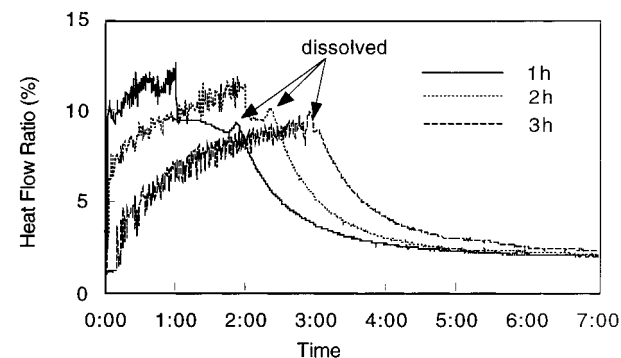


Figure 9. Heat flow curves measured for various addition periods at 30 °C with a 200 rpm stirring speed.

content increased). If the dissolution of **2** depended on the solvent components, the time for dissolution should be same. The addition periods were changed in the range 1–3 h although the times for dissolution after the end of addition were apparently different from each other (Figure 9). From these results, the dissolution of **2** was not affected by physical properties like agitation or solvent composition.

For all of the conditions shown in Figures 8 and 9, the conversion of **2** was about 55% at the dissolution point. From these results, the dissolution of **2** was affected by the reaction progress; that is, the reaction rate up to the conversion of 55% seemed to be equal to the rate of dissolution of **2** which was expressed by the Arrhenius equation of the measured heat flow curve. Therefore, the dissolution of **2** did not change with scale-up.

The reaction calorimeter was operated under isothermal conditions at different temperatures in the range 20–30 °C, and from the measured heat flow curves the rate constants were obtained by the Arrhenius plot (k_{dissolve} , Figures 10 and 11; Table 2). From these results, the heat rate could be expressed as in the equation in Chart 2.

The calculated heat production profile is as follows. The heat production rate is proportional to the dissolution rate until the conversion of **2** is 55%, after which the heat rate is proportional to the main reaction rate as shown in Chart 2. The dissolution rate and the main reaction rate were calculated using the kinetic parameters listed in Tables 1 and 2. We checked the reliability of these kinetic parameters by comparison of the actual and the calculated heat flow, and the result showed good agreement (Figure 12), so we

(4) Compound **2** is not very soluble in water (<0.005 g/mL at 20 °C) or methanol (0.5 g/mL at 20 °C), so the reaction was significantly influenced by the dissolution rate of **2**. To use more solvent volume in order to dissolve **2** was not good for production efficiency; using less solvent to increase efficiency caused the byproduct **3** to increase significantly because of high concentration.

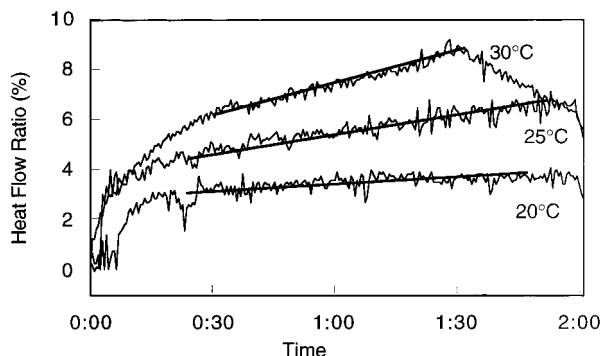


Figure 10. Heat flows at various temperatures and their slopes during 2 h addition with a 200 rpm stirring speed.

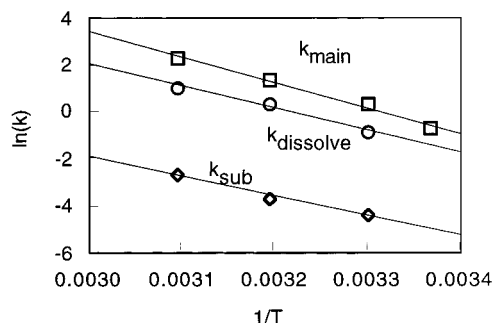


Figure 11. Arrhenius plot of the dissolution rate constants (k_{sub}) obtained from the slopes of heat flows measured by reaction calorimeter (Figure 10).

Table 2. Arrhenius regression analysis results on the rate of dissolution of **2**

	param	value	correlation coeff
k_{dissolve}	E_{a}	141.3 kJ/mol	0.9886
	A_0	2.34×10^{14} L/mol·h	

Chart 2. Equations for calculating the rate of heat production considering dissolution of **2**

$$\begin{aligned} \text{rate of heat production} &\cong (4.68 \times 10^{15})e^{10880/T} C_2 C_{\text{HNMe}_2} \\ &\quad (\text{conversion of } \mathbf{2} > 55\%) \\ &\cong (2.34 \times 10^{14})e^{11580/T} C_2 C_{\text{HNMe}_2} \\ &\quad (\text{conversion of } \mathbf{2} > 55\%) \end{aligned}$$

could use those for further simulation studies. When the slurry of **2** in methanol without aqueous dimethylamine was heated up to 50 °C and dissolved, of course, no reaction occurred and there was no exotherm or endotherm during the operation. Thus the heat production profile could be calculated without considering the dissolution itself.

Simulation Studies on the Optimization of the Reaction. In the simulation studies, the addition of dimethylamine was assumed to be operated under isothermal conditions and then the temperature was also to be maintained constant. The reaction was then judged to end when the conversion of **2** became less than 0.1%/h.

At first, we simulated the reaction from a quality point of view. On the basis of the kinetic parameters (Table 1), the yield of byproduct **3** was calculated at various temperatures and addition periods (Figure 13). When the operating temperature was under 25 °C, **3** was expected to be formed

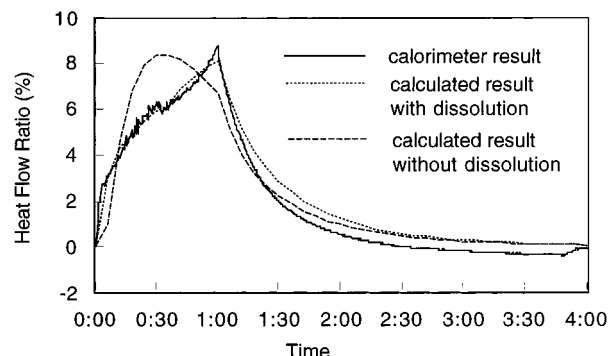


Figure 12. Predicted and actual heat flow of the reaction at 30 °C with a 1 h addition period: solid line (—), actual heat flow measured by reaction calorimeter; dotted line (···), heat flow calculated with eq 2 (considering dissolution); dashed line (---), heat flow calculated without considering dissolution.

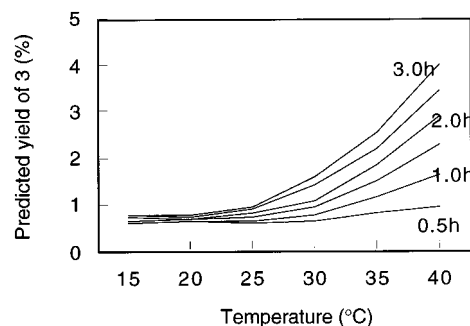


Figure 13. Predicted yield of **3** for various temperatures and addition periods.

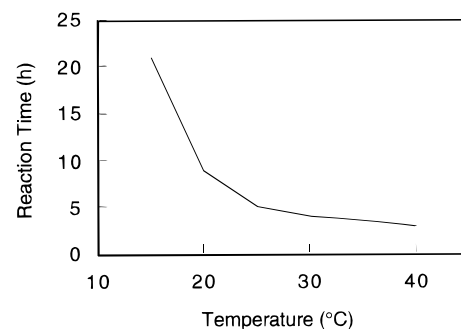


Figure 14. Predicted reaction time for various temperatures with a 1 h addition of aqueous dimethylamine.

at almost 1% in each addition period. Even when the temperature was 40 °C and the addition period was shorter than 1 h, the yield of **3** was expected to be less than 2%. At temperatures higher than 35 °C and addition periods greater than 2 h, the byproduct **3** would increase markedly.

The yield of **3** seemed to be reduced at low temperature, but the productivity of the product **1** became worse because of the slow reaction (Figure 14). On the basis of productivity and quality considerations, the reaction should be finished within 12 h and the formation of **3** should be less than 2%.⁵

The best temperature was thought to be about 25 °C. If the temperature was higher than 25 °C, the byproduct **3** would increase, and if the temperature was lower than 25 °C, the reaction would not end in 8 h.

(5) In the subsequent synthetic steps, the byproduct **3** is effectively removed when the yield of **3** is less than 3%.

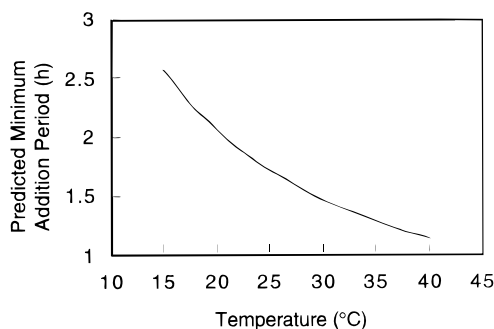


Figure 15. Predicted shortest addition period at various temperatures of actual plant reactor.

Chart 3. Equations for calculating the Damköhler number and T_{cf} equations

$$Da = \frac{2}{\pi} \frac{1}{(1-x)^2} = kC_{2\text{initial}}t$$

$$T_{cf} = T_r + \sqrt{\frac{2}{\pi(Da)}\Delta T_{ad}}$$

^a Da is the Damköhler number, x is the conversion of starting material **2**, k is the rate constant of the main reaction, $C_{2\text{initial}}$ is the concentration of **2** at the start of reaction, t is the reaction time, T_{cf} is the maximum temperature in the case of a cooling failure, T_r is the reaction temperature, ΔT_{ad} is the adiabatic temperature rise of this reaction (about 40 °C), and π is the circular constant.

In order to decrease the byproduct, the addition period should be short (Figure 13), but the minimum addition period depended on the cooling ability of the actual reactor. By considering the cooling ability, the shortest addition period for keeping the reaction at 25 °C was calculated to be 1.7 h⁶ (Figure 15). So we thought that the best set of conditions was addition of dimethylamine as rapidly as possible with the temperature kept at about 25 °C (1.7 h).

Next, we studied the reaction from a safety point of view. When the reaction was terminated, the time needed after the addition of dimethylamine and the heat accumulation was not clear (Figure 4). Therefore, we had to establish the conditions under which the heat accumulation would be lower. When the reaction temperature is low, the heat accumulation becomes large because of the slow reaction, and the maximum temperature in the case of a cooling failure (T_{cf}) will be high. On the other hand, when the reaction temperature is high, the heat accumulation becomes small, but it means that the starting temperature is high, so the T_{cf} also becomes high. In these cases, the T_{cf} can be calculated using the Damköhler number (Da), which is the dimensionless number for the reaction rate (Chart 3).⁷ According to the equations in Chart 3, the T_{cf} of this process could be calculated for various temperatures and addition periods (Figure 16). It was thought that the lower the T_{cf} is, the easier it is to control the reaction temperature if a cooling failure occurs, which provides more safety.

Using the best conditions from a quality point of view of “25 °C, 1.7 h addition” (yield of byproduct **3** was calculated to be 0.8% in this case), the T_{cf} was estimated as 59.6 °C. If

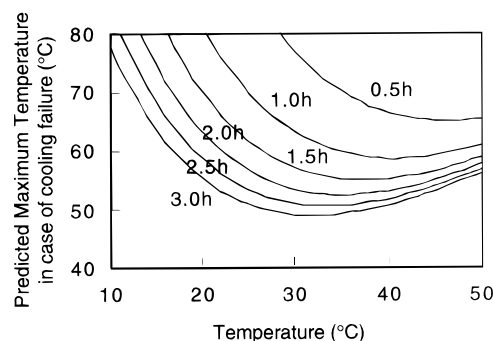


Figure 16. Maximum temperature of the reaction in case of a cooling failure (T_{cf}).

Table 3. Scale-up results of this reaction

scale	addn period, h	temp range, °C	yield, %	
			1	3
lab	~1	~30	90–95	0.3–0.8
plant	1.3	25–27	93.4	0.8

the cooling ability of the reactor was worse than the estimated cooling ability and/or the addition period became longer than 2 h, the yield of **3** was calculated to be 0.9% and the T_{cf} was calculated as 57.2 °C. When the temperature was 30 °C for the same addition period (1.7 h), the yield of **3** would be 0.9% and the T_{cf} would be 56.8 °C. These differences in the yield of **3** and the T_{cf} seemed not to be a severe problem in this process. Therefore, the temperature for the addition of dimethylamine could be between 25 and 30 °C.

Summary. We have simulated this process with high quality, high productivity, and safety in the plant by studying the reaction kinetics. After these studies, we did scale testing. For temperature control, we used partial brine flow (−5 °C) during and after the dimethylamine addition. The cooling ability of the reactor was better than estimated, and the addition period was shorter than 1.7 h, which were good for quality and productivity. The results are shown in Table 3.

In this case, we have studied only isothermal conditions, but expanding to nonisothermal conditions will make it possible to find an easier way to control the operation with high-quality product. We intend as the next step to simulate the process under nonisothermal conditions.

Experimental Section

All materials were commercially available. (3-Bromopropyl)triphenylphosphonium bromide (**2**) was purchased from Manac Incorporated (>97% purity), and MeOH and 50% aqueous dimethylamine were purchased from Ishizu Seiyaku, Ltd. For an analytical sample, the product, [3-(dimethylamino)propyl]triphenylphosphonium bromide (**1**), was purchased from Aldrich Co.

The analysis of the reaction was carried out using the HPLC internal standard method as described below. ¹H and ¹³C NMR spectra were recorded on a Bruker AC300 spectrometer with TMS as the internal standard. IR spectra were recorded on a Shimadzu FTIR-4300.

(6) The shortest addition period was calculated from the balance of the total heat production and the cooling capacity of the actual reactor in which this reaction was operated.

(7) (a) Hugo, P.; Steinbach, J.; Stoessel, F. *Chem. Eng. Sci.* **1988**, *43*, 2147.
(b) Stoessel, F. *Chem. Eng. Prog.* **1995**, *9*, 46.

HPLC Analysis. Column: YMC-Pack ODS-AM 312. 150 × 6 mm (YMC Co., Ltd.). Column temperature: 25 °C. Mobile phase: 1.5 L of H₂O, 1.0 L of CH₃CN, and 0.5 L of MeOH with 10.25 g of potassium dihydrogen phosphate and 6.5 g of sodium 1-octanesulfonate, pH 3.0 adjusted with 85% H₃PO₄. Flow rate: 1 mL/min. Detection: UV 225 nm. Internal standard: butyl *p*-hydroxybenzoate.

CHETAH Calculation. The CHETAH calculation was run with Version 7.0. CHETAH has no group value of salts such as **1–3**, so these compounds were calculated as free bases.

DSC Measurements. A MAC Science Co., Ltd., DSC3100 with a stainless steel cell was used under 2 kg/cm² pressure (air). The heating rate was 10 °C/min from 50 to 500 °C.

ARC Measurements. A Columbia Scientific Industries ARC with a titanium bomb was used as follows. Sample mass: 1–3 g. Thermal inertia factors (PHI factors): 1.7–3.9. Start temperature: 40 °C. End temperature: 405 °C. Slope sensitivity: 0.02 °C/min. Heat step temperature: 5 °C. Calculation step temperature: 0.2 °C. Wait time: 10 min.

Synthesis of *N,N*-Dimethyl-*N,N*-bis[3-(triphenylphosphonio)propyl]ammonium Tribromide (3**).** A mixture of 140.0 g (0.244 mol) of **2** and 96.0 g (0.244 mol) of **1** in 288 mL of MeOH was heated to reflux. After 14 h, the solvent was evaporated and the residue was crystallized from 400 mL of toluene. The crude crystal of **3** (192.3 g) was recrystallized from 500 mL of CH₃CN. Then 109.8 g of **3** was obtained with 98% purity (50% yield).

¹H NMR (CDCl₃–CD₃OD, 300 MHz): δ 2.16–2.33 (4H, m), 2.32 (6H, s), 3.75 (4H, t, *J* = 15.8 Hz), 4.25 (4H, t, *J* = 7.7 Hz), 7.65–7.96 (30 H, m).

¹³C NMR (CDCl₃–CD₃OD, 75 MHz): δ 19.6 (d), 17.1 (s), 50.7 (s), 63.7 (d), 117.4 (d), 130.7 (d), 134.1 (d), 135.2 (d).

IR (KBr, cm^{−1}): 3420, 1420, 1440, 1180, 1000, 740, 720, 690.

Determination of Reaction Constants. To a slurry of **2** (20.0 g, 43 mmol) in 28 mL of MeOH stirred at each reaction temperature was quickly added 50% aqueous

dimethylamine (2.8 equiv) which was preheated to each reaction temperature. The compound **2** dissolved after a few minutes. Every 20 min, 1 mL of the resultant solution was taken, to which was added 1 mL of 0.05 N HCl for quenching the reaction. After each sample was diluted to 10 mL with MeOH and mixed with the internal standard, the concentrations of the starting material **2**, the product **1**, and the byproduct **3** were analyzed by HPLC. The main reaction rate constant was obtained with correlation of the reaction time and the concentrations of the product **1** as follows: Considering first-order reaction, time was plotted for (*x* axis) as a function of the natural logarithm of the reciprocal of the remainder ratio of **1** (ln[1/(1 − *x*)] (*y* axis); the relation of these points was a linear correlation across the origin (correlation coefficient *r*² > 0.98), and the slope of the line showed the main reaction rate constant *k*_{main}.

As stated as above, the subreaction rate constant was obtained; thus 4.3 g (10 mmol) of **1** and 4.6 g (10 mmol) of **2** in 10 mL of MeOH (dissolved) were reacted at each reaction temperature. After the reaction was quenched, the concentrations of **1–3** were analyzed by HPLC.

Measurement of Heats of Reaction. Mettler's RC1 reaction calorimeter outfitted with an AP01 batch reactor (2 L glassware) was used. The starting material **2** (500 g) and MeOH (700 mL) were charged in the reactor, and the operating conditions (temperature, stirring speed) were determined. After the temperature was constant, 50% aqueous dimethylamine (2.8 equiv) at ambient temperature was proportionally added with a dosing pump over a set period. The measurement was continued till heat production ceased and the end of the reaction was determined by HPLC analysis. Calibrations for determining the heat capacity and the heat transfer coefficient were performed before and after the reaction. Values of heat production were cited per mole of **2**. Heat flow calculation terms included *Q*_{flow} (heat production), *Q*_{accum} (heat accumulation), *Q*_{dos} (heat flow due to dosing), and *Q*_{loss} (heat loss through the reactor cover).

Received for review October 28, 1997.

OP970055U